

Computational Grid Optimization for the 3D Higher-Order Parabolic Equation

Mikhail S. Lytaev(✉)

St. Petersburg Federal Research Center of the Russian Academy of Sciences, 14-th Linia, V.I., No. 39, Saint Petersburg 199178, Russia
mikelytaev@gmail.com

Abstract. This work is devoted to the wave propagation modeling in an essentially three-dimensional medium. Finite-difference Padé approximations of the three-dimensional one-way Helmholtz equation are considered. An algorithm for automatic mesh generation based on minimizing the dispersion error is proposed. The mesh is optimized in such a way as to minimize the computational complexity of the numerical scheme. It is shown that reference propagation constant affects the performance of the numerical scheme and a formula for its optimal value was derived. Approximations of the transversal operator of the second and fourth order of accuracy, the alternating-direction implicit (ADI) splitting method were considered. The optimal meshes were analyzed for various configurations of the numerical scheme, which allowed to quantify its possibilities and limitations. Automating the numerical scheme setup allows to prevent modeling errors and overspending of the computational resources.

Keywords: wave propagation · parabolic equation · mesh optimization · alternating-direction implicit · Padé approximation · Finite-difference

1 Introduction

The need for computer modeling of the wave field spatial distribution arises in various fields of mathematical physics: acoustics, radiophysics, geophysics, optics and quantum mechanics. Despite the different nature of the underlying physical phenomena, corresponding mathematical models are, in a certain sense, universal [22]. Accordingly, the numerical methods used to solve them can be reused in various applications.

One of such universal methods of the wave propagation theory is the parabolic equation (PE) method. It is usually used to compute the wave field in inhomogeneous waveguides. It was originally developed in 1946 by Leontovich and Fock [11] to tackle the tropospheric radio wave propagation problem. Then the PE method found wide application in computational sonar problems [9]. Various modifications and effective numerical schemes appeared, which were then used

© The Author(s), under exclusive license to Springer Nature Switzerland AG 2023
O. Gervasi et al. (Eds.): ICCSA 2023, LNCS 13956, pp. 170–185, 2023.
https://doi.org/10.1007/978-3-031-36805-9_12

in optics [3] and seismology [5]. There are also a number of theoretical papers [2,21], where, in particular, the connection between the PE and the Helmholtz equation is revealed [6,7]. Owing to these studies, in this paper terms "parabolic equation" and "one-way Helmholtz equation" are used as synonyms. Basically, the PE method is used in a two-dimensional environment, but recently there has been increasing interest in its application in essentially three-dimensional problems. In [12,19,24] it is proposed to use the PE method to compute the radio wave field in tunnels. In [8,15,16], the PE method is used to compute the radio wave propagation in dense urban conditions. There are more and more works devoted to modeling the acoustic field in a three-dimensional inhomogeneous underwater environment [10,13,20].

The main problems with the numerical solving of the three-dimensional PE are the low computation speed and the huge memory requirements. In part, this problem can be tackled by applying the higher-order approximations and the transverse operator splitting using the alternating direction implicit [18] (ADI) method. Meanwhile, the issue of the automatic selection of the computational grid and other artificial parameters in an optimal way is relevant. Indeed, using a grid that is too dense will lead to overspending of the computational resources, and computing on an insufficiently dense grid will yield an incorrect results. Currently, there is no general theory of choosing the optimal computational parameters of a numerical scheme. They are usually selected manually by an expert based on some empirical considerations.

Previously, the optimization problem of the finite-difference PE approximation was solved for the two-dimensional case in a homogeneous [17] and inhomogeneous medium [14]. The aim of this paper is to develop a method for optimizing a finite-difference numerical scheme for the three-dimensional PE and analyze optimal grids under various configurations. In this paper, by optimization we mean reducing the required computing time and memory without increasing the computing resources. It should also be mentioned work [23], where it is proposed to jointly use the Padé approximation of the propagation operator along the longitudinal coordinate and the 4th order approximation of the transversal operator. The analysis of the scheme accuracy depending on the approximation order and the propagation angle was also carried out in [23].

The paper is organized as follows. In the next section, the mathematical formulation of the problem is posed and the one-way Helmholtz equation in the spectral domain is derived. Section 3 is devoted to the numerical scheme under consideration. In Sect. 4, the discrete dispersion relations are derived, on the basis of which the algorithm for optimizing the computational grid is constructed in Sect. 5. Section 6 presents and analyzes optimization results for various configurations.

2 3D PE

Consider the following three-dimensional scalar Helmholtz equation defined in the Cartesian coordinate system

$$\frac{\partial^2\psi}{\partial x^2}+\frac{\partial^2\psi}{\partial y^2}+\frac{\partial^2\psi}{\partial z^2}+k^2\psi=0, \tag{1}$$

where $\psi(x,y,z)$ is the wave field distribution to be determined, $k=2\pi f/c$ is the wavenumber, f is the radiation frequency, c is the wave propagation speed.

The wave propagation process is generated by the initial condition

$$\psi(0,y,z)=\psi_0(y,z)$$

where $\psi_0(y,z)$ in known function, which corresponds to the radiation source.

Function $\psi(x,y,z)$ may be subject to additional boundary and radiation conditions, which, however, do not matter for the present study.

It is further assumed that the wave propagation process occurs mainly in the positive direction of the x axis.

We introduce into consideration the two-dimensional Fourier transform of function ψ with respect to variables y and z

$$\tilde{\psi}(x,k_y,k_z)=\frac{1}{2\pi}\int\limits_{-\infty}^{+\infty}\int\limits_{-\infty}^{+\infty}\psi(x,y,z)e^{-ik_z z-ik_y y}dydz,$$

and inverse Fourier transform

$$\psi(x,y,z)=\frac{1}{2\pi}\int\limits_{-\infty}^{+\infty}\int\limits_{-\infty}^{+\infty}\tilde{\psi}(x,k_y,k_z)e^{ik_z z+ik_y y}dk_y dk_z.$$

Note that the Fourier transform in this case has the physical meaning of decomposing the wave field into the plane waves with transversal wavenumbers k_y and k_z.

Applying the above transformation to Eq. (1), we obtain the following equation

$$\frac{\partial^2\tilde{\psi}}{\partial x^2}-k_y^2\tilde{\psi}-k_z^2\tilde{\psi}+k^2\tilde{\psi}=0. \tag{2}$$

Equation (2) may be rewritten as follows

$$\left[\frac{\partial}{\partial x}-i\sqrt{-k_y^2-k_z^2+k^2}\right]\left[\frac{\partial}{\partial x}+i\sqrt{-k_y^2-k_z^2+k^2}\right]\tilde{\psi}=0.$$

The latter equation has the physical meaning of decomposition into waves propagating in the positive and negative directions along the x axis. Next, we are only interested in waves propagating in the positive direction, so we consider the following equation

$$\left[\frac{\partial}{\partial x}-i\sqrt{-k_y^2-k_z^2+k^2}\right]\tilde{\psi}=0. \tag{3}$$

3 Numerical Solution

The numerical solution is sought on a uniform grid with steps Δx, Δy and Δz. It is usually assumed that $\Delta y = \Delta z$. The following notation is further used

$$\psi_{i,j}^{n} = \psi\left(n\Delta x, i\Delta y, j\Delta z\right).$$

The number of grid nodes along each coordinate is denoted respectively as n_x, n_y and n_z.

3.1 Padé Approximation of the Propagator

Let's use the following replacement

$$u(x, y, z) = e^{-i\beta x}\psi(x, y, z), \tag{4}$$

where β is the reference propagation constant, which sense will be clarified in the next sections.

The step-by-step solution can be written as follows

$$\tilde{u}\left(x + \Delta x, k_y, k_z\right) = \exp\left(i\beta\Delta x\left(\sqrt{1+\xi} - 1\right)\right)\tilde{u}\left(x, k_y, k_z\right), \tag{5}$$

where

$$\xi = -\frac{k_y^2}{\beta^2} - \frac{k_z^2}{\beta^2} + \frac{k^2}{\beta^2} - 1. \tag{6}$$

Following [4], we apply the Padé approximation [1] of order $[m/n]$ in the vicinity of $\xi = 0$ to the propagation operator (5)

$$\exp\left(ik\Delta x\left(\sqrt{1+\xi} - 1\right)\right) \approx \frac{1 + \sum_{l=1}^{m}\tilde{a}_l\xi^l}{1 + \sum_{l=1}^{n}\tilde{b}_l\xi^l} = \prod_{l=1}^{p}\frac{1 + a_l\xi}{1 + b_l\xi}, \tag{7}$$

where a_l and b_l are the Padé approximation coefficients.

Now the action of propagation operator (5) in the spectral domain can be written using auxiliary functions v_l as follows

$$\begin{cases} \left(1 + b_1\xi\right)\tilde{v}_1^n = \left(1 + a_1\xi\right)\tilde{u}^{n-1} \\ \left(1 + b_l\xi\right)\tilde{v}_l^n = \left(1 + a_l\xi\right)\tilde{v}_{l-1}^n \qquad l = 2\ldots p-1 \\ \ldots \\ \left(1 + b_p\xi\right)\tilde{u}^n = \left(1 + a_p\xi\right)\tilde{v}_{p-1}^n. \end{cases} \tag{8}$$

Applying the inverse Fourier transform, we obtain a system of two-dimensional differential equations in the spatial domain (y, z)

$$\begin{cases} \left(1 + b_1 L\right)v_1^n = \left(1 + a_1 L\right)u^{n-1} \\ \left(1 + b_l L\right)v_l^n = \left(1 + a_l L\right)v_{l-1}^n \qquad l = 2, \ldots, p-1 \\ \ldots \\ \left(1 + b_p L\right)u^n = \left(1 + a_p L\right)v_{p-1}^n, \end{cases} \tag{9}$$

with transversal operator

$$Lu = \frac{1}{\beta^2}\frac{\partial^2 u}{\partial y^2} + \frac{1}{\beta^2}\frac{\partial^2 u}{\partial z^2} + \left(\frac{k^2}{\beta^2} - 1\right) u. \tag{10}$$

3.2 Approximation of the Transversal Operator

Next, we need to construct a numerical approximation of the transversal operator (10). The second derivatives will be approximated by the following 4th order 3-point scheme

$$\frac{\partial^2 u}{\partial z^2} \approx D_{\Delta z} u = \frac{1}{\Delta z^2}\delta_z^2 \left(1 + \alpha\delta_z^2\right)^{-1} u,$$

where $\alpha = 0$ for the 2nd order scheme and $\alpha = 1/12$ for the 4th order one. Second difference operator is defined as follows

$$\delta_{\Delta z}^2 = u\left(z - \Delta z\right) - 2u\left(z\right) + u\left(z + \Delta z\right).$$

The approximation of the second derivative along y is written similarly.

Now the approximation of operator L can be written as follows

$$Lu \approx L_d u = \frac{1}{\beta^2} D_{\Delta y} u + \frac{1}{\beta^2} D_{\Delta z} + \left(\frac{k^2}{\beta^2} - 1\right) u. \tag{11}$$

Setting $\Delta y, \Delta z \to 0$, one can achieve an arbitrarily accurate approximation. However, substitution such an approximation into each line of system (9) yield a system of linear algebraic equations with dimension $n_y n_z \times n_y n_z$. Sparsity matrix of such a system depicted at Fig. 1. Given its sparsity, the specified system can be solved in $O\left(\left(n_y n_z\right)^2\right)$ operations.

The solution of the above mentioned system can be too time and memory consuming for practical problems, so an approximate approach of splitting operator L into two operators that are applied sequentially has been proposed [18]

$$L_d^{ADI} u = \left[\frac{1}{\beta^2} D_{\Delta y} + \frac{1}{2}\left(\frac{k^2}{\beta^2} - 1\right)\right]\left[\frac{1}{\beta^2} D_{\Delta z} + \frac{1}{2}\left(\frac{k^2}{\beta^2} - 1\right)\right] u. \tag{12}$$

This approach is called an Alternating-direction implicit (ADI) method [24] and allows to get an approximate solution faster, namely in $O\left(n_y n_z\right)$ operations. Further, it will be shown that the splitting error increases with the growth of the propagation angle and, in fact, this approximation is not applicable at large propagation angles.

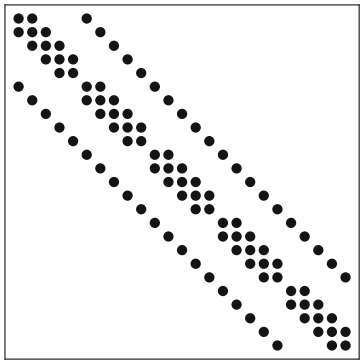

Fig. 1. Sparsity matrix.

4 Dispersion Relations

Consider a three-dimensional plane wave

$$\phi(x, y, z) = \exp(-ik_x x - ik_y y - ik_z z), \tag{13}$$

where

$$k_x = k\cos\theta, \tag{14}$$

$$k_y = k\cos\varphi\sin\theta,$$

$$k_z = k\sin\varphi\sin\theta,$$

θ is the angle between the positive direction of the x axis and the direction of the plane wave (further denoted as propagation angle), φ is the angle between the y axis and the projection of the plane wave direction onto the yz plane. Further we assume that $\varphi \in [0, 2\pi]$, $\theta \in [0, \theta_{max}]$, $\theta_{max} \in [0, \pi/2]$ is the maximum propagation angle for a particular problem, selected based on geometric considerations [14].

Substituting plane wave (13) into numerical scheme (9), (11), we obtain the following expression for the discrete longitudinal wavenumber [3,24]

$$\tilde{k}_x(\Delta x, \Delta y, \Delta z, a_1 \dots a_p, b_1 \dots b_p, \theta, \varphi) = k + \frac{\ln \prod_{l=1}^{p} t_l}{i\Delta x},$$

where

$$t_l = \frac{1 + a_l(\xi_d^y + \xi_d^z)}{1 + b_l(\xi_d^y + \xi_d^z)},$$

$$\xi_d^y = -\frac{1}{\beta^2 \Delta y^2} \sin^2\left(\frac{k_y \Delta y}{2}\right) - \frac{4\alpha}{\beta^2 \Delta y^2} \sin^4\left(\frac{k_y \Delta y}{2}\right) + \frac{1}{2}\left(\frac{k^2}{\beta^2} - 1\right),$$

$$\xi_d^z = -\frac{1}{\beta^2 \Delta z^2} \sin^2\left(\frac{k_z \Delta z}{2}\right) - \frac{4\alpha}{\beta^2 \Delta z^2} \sin^4\left(\frac{k_z \Delta z}{2}\right) + \frac{1}{2}\left(\frac{k^2}{\beta^2} - 1\right).$$

Performing a similar operation for a numerical scheme with splitting (9), (12), we get a slightly different expression for t_l

$$t_l = \frac{(1 + a_l \xi_d^y)(1 + a_l \xi_d^z)}{(1 + b_l \xi_d^y)(1 + b_l \xi_d^z)}.$$

The following rough estimate

$$|\,[1 + a_l(\xi_d^y + \xi_d^z)] - (1 + a_l \xi_d^y)(1 + a_l \xi_d^z)\,| = |a_l^2 \xi_d^y \xi_d^z|$$

indicates that the splitting-related error grows with increasing k_y and k_z. At the same time, setting $\Delta y, \Delta z \to 0$ will not reduce the error. Thus, ADI is a small-angle approximation and is inapplicable at large propagation angles regardless of the approximation order and the mesh density. Approach to overcome this issue was made in [3], where an iterative ADI method was proposed.

5 Optimization Algorithm

It is further assumed that maximum propagation angle θ_{max}, as well as the acceptable error ε at the distance x_{max} from the propagation staring point are given.

5.1 Optimizing of the Reference Propagation Constant

Previously in (4) we introduced artificial parameter β, called the reference propagation constant. The most common choice of its value is $\beta = k$. Although the specific value of this parameter does not affect the derivation and validity of the numerical scheme, we will show further that it can be chosen in an optimal way.

Consider the error of rational approximation (7)

$$R(\xi) = |\exp\left(ik\Delta x\left(\sqrt{1+\xi} - 1\right)\right) - \prod_{l=1}^{p} \frac{1 + a_l \xi}{1 + b_l \xi}|.$$

Figure 2 demonstrates the dependence of R on ξ when $\Delta x = 25\,\mathrm{m}$, Padé order is [6/7]. In can be seen that since Padé approximation is local, the minimum error is localized in the vicinity of point $\xi = 0$ and monotonically increases with distance from the specified point. A similar behavior is observed for other

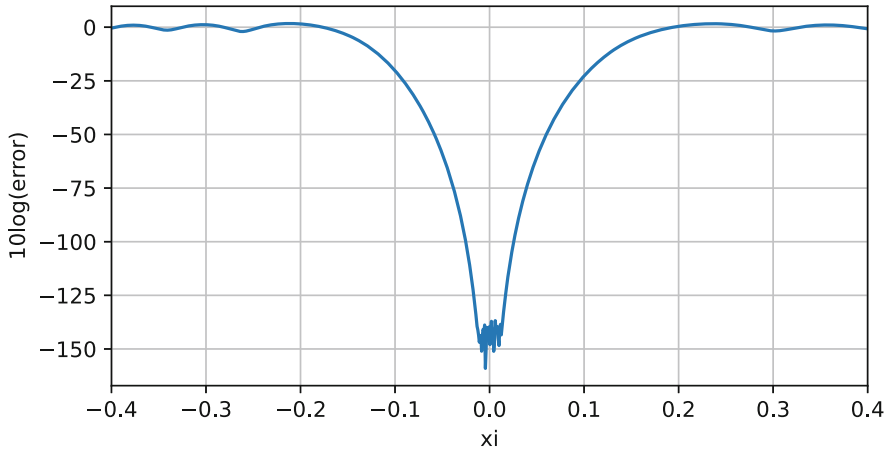

Fig. 2. The dependence of rational approximation error R on ξ when $\Delta x = 25\,\text{m}$, Padé order is [6/7].

values of Δx and approximation orders. Keeping in mind formulas (6) and (14), variable ξ can be expressed via propagation angle θ and propagation constant β as follows

$$\xi = -\frac{k^2}{\beta^2}\sin^2\theta + \frac{k^2}{\beta^2} - 1.$$

Then the set of its possible values will take the form

$$\xi \in \left[-\frac{k^2}{\beta^2}\sin^2\theta_{max} + \frac{k^2}{\beta^2} - 1, \frac{k^2}{\beta^2} - 1\right]. \tag{15}$$

For example, if one select the standard value $\beta = k$, then according to (15), the values $\xi \in [-\sin^2\theta_{max}, 0]$, i.e. will always be negative. So the Padé approximation at $\xi > 0$ turns out to be unused. Considering this observation, it would be reasonable to choose such a value of β, at which the range of values of ξ most fully falls into the neighborhood of point $\xi = 0$. To do this, we write the following equality

$$-\left(-\frac{k^2}{\beta^2}\sin^2\theta_{max} + \frac{k^2}{\beta^2} - 1\right) = \frac{k^2}{\beta^2} - 1,$$

from which we van easily get the following optimal value of the propagation constant

$$\beta = \frac{2\pi f}{c}\sqrt{\frac{2 - \sin^2\theta_{max}}{2}}. \tag{16}$$

5.2 Mesh Optimization

Following [14,17], we formulate the computational grid optimization problem. It is required to maximize the cell sizes of the computational grid so that the dispersion error at a given distance x_{max} does not exceed some ε. Using the previously obtained discrete dispersion relation and bearing in mind that the asymptotic complexity of the numerical scheme under consideration is $O\left(n_x \left(n_y n_z\right)^2\right)$, we get the following conditional optimization problem

$$\Delta x \left(\Delta y \Delta z\right)^2 \to \max$$

under condition

$$n_x \tau < \varepsilon, \tag{17}$$

where τ means the dispersion error at one step by x

$$\tau = \max_{\theta \in [0, \theta_{max}], \varphi \in [0, 2\pi]} |\tilde{k}_x - k \cos\theta|,$$

$n_x = \lceil x_{max}/\Delta x \rceil$ is the number of required steps along x axis. This algorithm takes into account the total accumulation of the dispersion error with each step along x axis.

Given the small dimension of this optimization problem and the fact that the steps along the transverse coordinates can be set equal ($\Delta y = \Delta z$), the problem is solved effectively by simply iterating over the reasonable values of cell sizes.

6 Optimization Results

This section presents the results of the proposed optimization algorithm under various conditions. In all examples we set $k = 2\pi$, $\varepsilon = 10^{-2}$.

6.1 Reference Propagation Constant Impact

First, let's evaluate how the value of parameter β affects the cell sizes. We will compare the standard value of β, equal to the wavenumber k, and the value obtained using proposed formula (16). Table 1 demonstrates the comparison of the optimal cell sizes for various values of θ_{max} and x_{max}. The gain is calculated as the ratio of asymptotic complexities

$$Gain = \frac{\Delta x_2 \left(\Delta y_2 \Delta z_2\right)^2}{\Delta x_1 \left(\Delta y_1 \Delta z_1\right)^2},$$

in other words, it shows how many times the proposed method is faster than the standard one. It is clearly seen that the proposed optimal value of β allows to reduce the computing time by 4–6 times. In addition, it follows from the results that with increasing θ_{max}, an increasingly dense computational grid is required. A decrease in longitudinal step Δx with an increase in θ_{max} leads to

an increase in n_x, which makes condition (17) unfeasible at large propagation angles. The proposed method of optimizing β allows to increase the maximum allowable angle by about 10°.

Figure 3 demonstrates the dependence of the discrete dispersion relation error on angle θ when $\Delta x = 7$ m, $\Delta y = \Delta z = 0.09$ m, Padé order is [6/7] and $\theta_{max} = 30°$. It can be seen that with the same computational parameters, standard value $\beta = k$ allows to account only angles up to 22°, while the proposed method can give precise results at angles up to 30°.

Table 1. Comparison of the optimal cell sizes. In all examples Padé order is [6/7], 4th order approximation is used for the transversal operator, splitting is not used. "-" means that a reasonable grid cannot be constructed for the given parameters.

$\theta_{max}(°)$	x_{max} (m)	$\beta = k$		Optimal β		Gain
		Δx_1 (m)	$\Delta y_1 = \Delta z_1$ (m)	Δx_2 (m)	$\Delta y_2 = \Delta z_2$ (m)	
3	10000	370	4.3	700	5.2	4.0
5	1000	130	2.8	245	3.4	4.1
10	1000	32.5	0.7	65.5	0.8	3.6
20	1000	8.2	0.16	15.5	0.19	3.76
30	1000	3.7	0.08	7.0	0.09	3.88
45	1000	1.6	0.034	3.02	0.04	3.61
60	100	1.0	0.03	1.6	0.04	6.17
70	100	-	-	1.0	0.025	-
80	10	-	-	-	-	-

6.2 Impact of the Operator Splitting

Next, let's consider how the splitting of operator L using the ADI method affects the accuracy of the numerical scheme. Table 2 presents the optimal values of the grid cell sizes for the ADI method and approximation without splitting. There are practically no differences in the required mesh, however, the proposed optimization method indicates that meshes for the ADI method that satisfy any feasible precision requirements do not exist when $\theta_{max} > 10°$. This is due to the splitting error, which increases with increasing propagation angle.

Figure 4 depicts the two dimensional distribution of the discrete dispersion error. It can be seen that when using the scheme without splitting, the minimum error is observed when $k_y, k_z = 0$ and monotonously increases in all directions as moving from this point. The ADI scheme gives a much larger error, while the location of areas with minimal error depends on the value of β.

6.3 Comparison of the 2nd and 4th Order Schemes

Now we will quantitatively estimate what performance gain is provided by using the 4th order accuracy scheme for approximating the derivatives in transverse

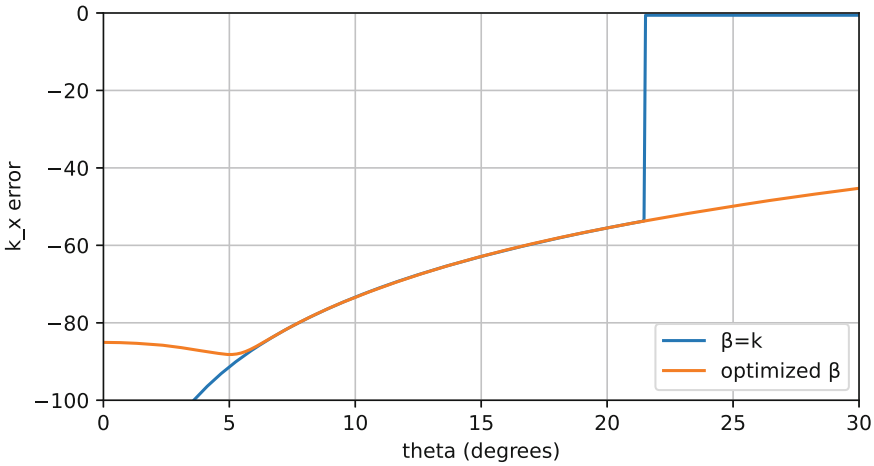

Fig. 3. Dependence of the discrete dispersion relation error ($10 \log |\tilde{k}_x - k_x|$) on angle θ when $\Delta x = 7$ m, $\Delta y = \Delta z = 0.09$ m, Padé order is [6/7], $\theta_{max} = 30°$. 4th order approximation is used for the transversal operator, splitting is not used.

Table 2. Comparison of the optimal cell sizes. In all examples Padé order is [6/7], 4th order approximation is used for the transversal operator, value of β is computed by formula (16). "-" means that a reasonable grid cannot be constructed for the given parameters.

$\theta_{max}(°)$	x_{max} (m)	Splitting (ADI)		No splitting	
		Δx (m)	Δz (m)	Δx (m)	Δz (m)
3	10000	700	5.2	700	5.2
5	1000	245	3.4	245	3.4
10	1000	65.5	0.9	65.5	0.82
20	1000	-	-	15.5	0.19
30	1000	-	-	7.0	0.09

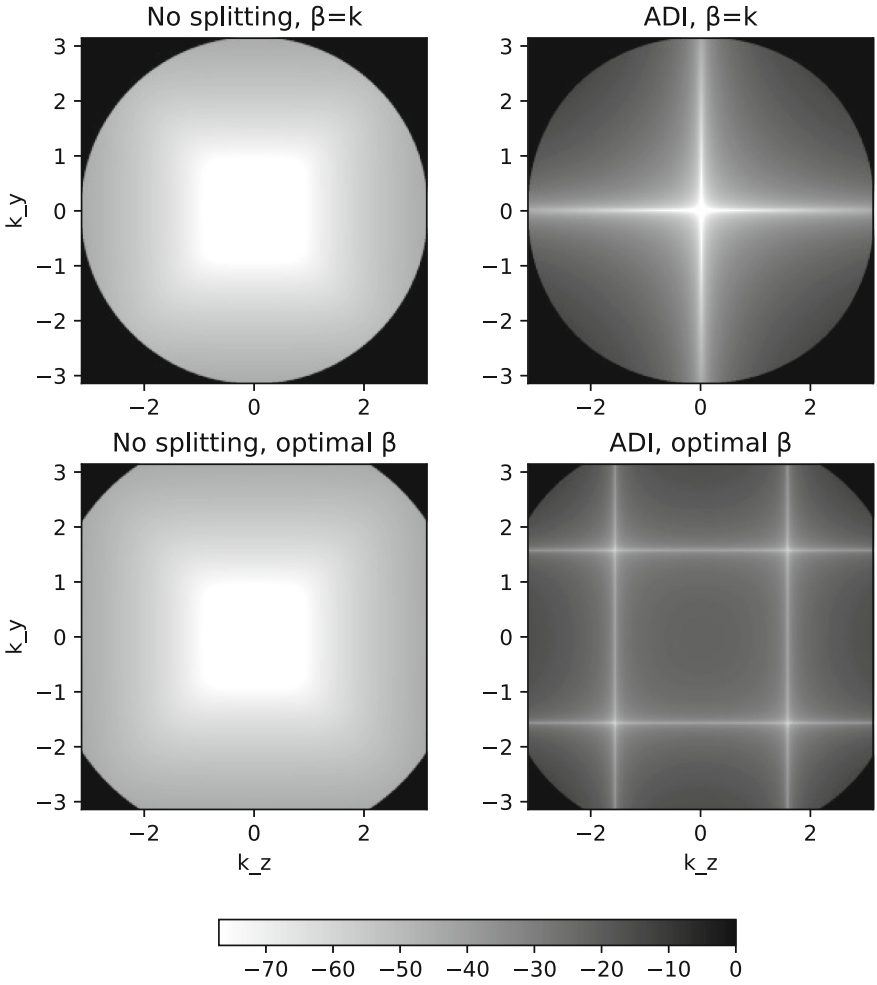

Fig. 4. Two dimensional distribution of the discrete dispersion error ($10 \log |\tilde{k}_x - k_x|$). In all examples $\Delta x = 3.7$ m, $\Delta z = 0.08$ m, $\theta_{max} = 30°$, Padé order is [6/7], 4th order approximation is used for the transversal operator.

operator L. Source data of the Table 3 is analogous to Table 2, but the optimal grid is computed for the 2nd order accuracy scheme ($\alpha = 0$). Comparing the both tables, it is clearly seen that the 4th order scheme allows using a more sparse grid along y and z axes, while the difference between the methods grows as the propagation angle increases. The gain in this case is considered between the 2nd and 4th order schemes. Density reduction is especially important for a non-splitting scheme, given its asymptotic complexity.

Table 3. Same as Table (2), but the 2nd order approximation order ($\alpha = 0$) was used instead.

$\theta_{max}(^\circ)$	x_{max} (m)	Splitting (ADI)			No splitting		
		Δx (m)	Δz (m)	Gain	Δx (m)	Δz (m)	Gain
3	10000	700	2.8	3.44	700	2.8	11.9
5	1000	245	1.9	3.2	245	1.9	10.6
10	1000	65.5	0.3	8.05	65.5	0.25	115.7
20	1000	-	-	-	15.5	0.03	1411.1
30	1000	-	-	-	7.0	0.009	10451.9

6.4 Comparison of Various Padé approximation orders

In the last example, we will investigate how the order of the Padé approximation affects the efficiency of the numerical scheme. It should be borne in mind that increasing the Padé approximation order leads not only to an increase in accuracy, but also to an increase in the number of rows in system (9), which in turn means an increase in the amount of computations. To evaluate the effectiveness in view of the approximation order, we introduce the following metric

$$V = \frac{p}{\Delta x \left(\Delta y \Delta z\right)^2} \sim p n_x \left(n_y n_z\right)^2 .$$

The smaller the value of V, the more efficient the algorithm is.

Table 4 shows the optimal meshes and values of V for the various approximation orders and propagation angles. It can be seen that choosing a large approximation order does not always turn out to be a winning strategy. For example, for $\theta_{max} = 3^\circ$ the optimal order is [2/3], and for $\theta_{max} = 10^\circ$ and $\theta_{max} = 20^\circ$ it makes no sense to take order greater than [5/6]. However, too small approximation order may not be applicable for the large propagation angles. In particular, it can be seen that it is impossible to find a reasonable mesh for $\theta_{max} = 20^\circ$ and order [1/1].

Table 4. Comparison of the optimal cell sizes. In all examples the 4th order approximation is used for the transversal operator, value of β is computed by formula (16). "-" means that a reasonable grid cannot be constructed for the given parameters.

$\theta_{max}(^\circ)$	x_{max} (m)	Order	Δx (m)	$\Delta y = \Delta z$ (m)	V(lower is better)
3	10000	[1/1]	130	1.9	6.0E−4
		[2/3]	730	5.2	5.62E−6
		[5/6]	700	5.2	1.17E−05
		[6/7]	700	5.2	1.36E−5
		[7/8]	700	5.2	1.56E−5
10	1000	[1/1]	0.8	0.16	1907
		[2/3]	47.5	0.64	0.37
		[5/6]	65.5	0.82	0.2
		[6/7]	65.5	0.82	0.23
		[7/8]	65.5	0.82	0.27
20	1000	[1/1]	-	-	-
		[2/3]	5.8	0.13	1811.0
		[5/6]	16.0	0.19	287.7
		[6/7]	16.0	0.19	335.7
		[7/8]	16.0	0.19	383.7

7 Conclusion

From a theoretical point of view, the proposed mesh optimization method provides a rigorous quantitative approach to evaluating various configurations of the finite-difference approximation. In particular, it gives an opportunity to clearly justify the optimal choice of the reference propagation constant. The method allows to evaluate the accuracy of the scheme as a whole, not just its separate steps.

From a practical point of view, the proposed method makes it possible to reduce the influence of the human factor on the modeling process, since artificial computational parameters are selected automatically. It gives an opportunity to eliminate the modeling errors due to an incorrectly selected computational grid, and also eliminates the overspending of the computational resources due to the choice of an unreasonably dense computational grid. In addition, being automated and not requiring expert intervention, numerical schemes can be more deeply integrated into complex software systems.

In this study, the case of constant velocity c was considered, but it can also be generalized to an inhomogeneous medium. In further research, it is planned to consider the optimization problem in relation to specific subject areas: radiophysics, computational underwater acoustics, seismology, optics.

Acknowledgments. This study was supported by the Russian Science Foundation grant No. 21-71-00039.

References

1. Baker, G.A., Graves-Morris, P.: Padé Approximants, vol. 59. Cambridge University Press (1996)
2. Bamberger, A., Engquist, B., Halpern, L., Joly, P.: Higher order paraxial wave equation approximations in heterogeneous media. SIAM J. Appl. Math. **48**(1), 129–154 (1988)
3. Bekker, E.V., Sewell, P., Benson, T.M., Vukovic, A.: Wide-angle alternating-direction implicit finite-difference beam propagation method. J. Light. Technol. **27**(14), 2595–2604 (2009)
4. Collins, M.D.: A split-step Padé solution for the parabolic equation method. J. Acoust. Soc. Am. **93**(4), 1736–1742 (1993)
5. Collins, M.D., Siegmann, W.L.: Parabolic equation techniques for seismology, Seismo-acoustics, and arctic acoustics. J. Theor. Comput. Acoust. **29**(02), 2130003 (2021)
6. Fishman, L., de Hoop, M.V., Van Stralen, M.J.N.: Exact constructions of square-root Helmholtz operator symbols: the focusing quadratic profile. J. Math. Phys. **41**(7), 4881–4938 (2000)
7. Fishman, L., McCoy, J.J.: Derivation and application of extended parabolic wave theories. I. factorized Helmholtz equation. J. Math. Phys. **25**(2), 285–296 (1984)
8. Janaswamy, R.: Path loss predictions in the presence of buildings on flat terrain: a 3-D vector parabolic equation approach. IEEE Trans. Antennas Propag. **51**(8), 1716–1728 (2003)
9. Jensen, F.B., Kuperman, W.A., Porter, M.B., Schmidt, H.: Computational Ocean Acoustics. Springer, New York (2014). https://doi.org/10.1007/978-1-4419-8678-8
10. Kozitskiy, S.: Coupled-mode parabolic equations for the modeling of sound propagation in a shallow-water waveguide with weak elastic bottom. J. Mar. Sci. Eng. **10**(10), 1355 (2022)
11. Leontovich, M.A., Fock, V.A.: Solution of the problem of propagation of electromagnetic waves along the Earth's surface by the method of parabolic equation. J. Phys. USSR **10**(1), 13–23 (1946)
12. Li, Y.S., Bian, Y.Q., He, Z., Chen, R.S.: EM pulse propagation modeling for tunnels by three-dimensional ADI-TDPE method. IEEE Access **8**, 85027–85037 (2020)
13. Lin, Y.T., Porter, M.B., Sturm, F., Isakson, M.J., Chiu, C.S.: Introduction to the special issue on three-dimensional underwater acoustics. J. Acoust. Soc. Am. **146**(3), 1855–1857 (2019)
14. Lytaev, M.: Mesh optimization for the acoustic parabolic equation. J. Mar. Sci. Eng. **11**(3), 496 (2023)
15. Lytaev, M., Borisov, E., Vladyko, A.: V2I propagation loss predictions in simplified urban environment: a two-way parabolic equation approach. Electronics **9**(12), 2011 (2020)
16. Lytaev, M.S.: Higher-order 3D parabolic equation for radio wave propagation modeling in a street canyon. In: 2019 IEEE Conference of Russian Young Researchers in Electrical and Electronic Engineering (EIConRus), pp. 873–876. IEEE (2019)

17. Lytaev, M.S.: Automated selection of the computational parameters for the higher-order parabolic equation numerical methods. In: International Conference on Computational Science and Its Applications 2020 (12249), pp. 296–311 (2020)
18. Marchuk, G.I.: Splitting and alternating direction methods. Handb. Numer. Anal. **1**, 197–462 (1990)
19. Martelly, R., Janaswamy, R.: An ADI-PE approach for modeling radio transmission loss in tunnels. IEEE Trans. Antennas Propag. **57**(6), 1759–1770 (2009)
20. Petrov, P., Katsnelson, B., Li, Z.: Modeling techniques for underwater acoustic scattering and propagation (including 3D effects). J. Mar. Sci. Eng. **10**(9), 1192 (2022)
21. Petrov, P.S., Ehrhardt, M., Trofimov, M.: On decomposition of the fundamental solution of the Helmholtz equation over solutions of iterative parabolic equations. Asymptot. Anal. **126**(3–4), 215–228 (2022)
22. Samarskii, A.A., Mikhailov, A.P.: Principles of Mathematical Modelling: Ideas, Methods, Examples. Taylor and Francis, Oxford (2002)
23. Wu, X., Li, Z., Liang, Z., Long, Y.: Higher-order FD-Padé scheme for 3D parabolic equation in radio-wave propagation. IEEE Antennas Wireless Propag. Lett. (2023)
24. Zhang, X., Sarris, C.D.: Error analysis and comparative study of numerical methods for the parabolic equation applied to tunnel propagation modeling. IEEE Trans. Antennas Propag. **63**(7), 3025–3034 (2015)